

Order parameter and critical exponent for the pressure-induced phase transitions in ReO_3

J.-E. Jørgensen* and J. D. Jorgensen

Materials Science and Technology Division, Argonne National Laboratory, Argonne, Illinois 60439

B. Batlogg and J. P. Remeika

AT&T Bell Laboratories, Murray Hill, New Jersey 07974

J. D. Axe

Brookhaven National Laboratory, Upton, New York 11973

(Received 22 July 1985)

Neutron powder diffraction data for ReO_3 show a sequence of phase transitions starting at 5 kbar consistent with the condensation of M_3 phonons. The structure is cubic $Pm3m$ at ambient pressure, tetragonal $P4/mbm$ at 5.2 kbar, and cubic $Im3$ at 7.3 kbar and higher pressures. A single order parameter, the rotation angle of the ReO_6 octahedra, describes the distortion in the high-pressure phases. The rotation angle varies as $(P - P_c)^\beta$ with $\beta = 0.322(5)$ over the entire pressure range of the measurements 5.0 to 27.4 kbar. This value of β indicates an unusually large critical region extending to rotation angles of more than 14° .

INTRODUCTION

ReO_3 has the nondistorted perovskite structure at ambient pressure. It is unique among the perovskites (which have the general formula ABO_3) because the usually occupied A sites are empty in ReO_3 . Furthermore, ReO_3 has metallic conductivity. A pressure-induced phase transition in ReO_3 was first discovered by Razavi *et al.*¹ who observed nonlinear behavior of the Fermi-surface cross sections at low temperatures at pressures close to 3 kbar. Schirber and Morosin² determined the critical pressure P_c to be 2.4 kbar at 2 K by de Haas-van Alphen measurements and proposed the name "compressibility collapse" for this transition because x-ray diffraction at room temperature showed that the compressibility is an order of magnitude larger in the high-pressure phase.

High-precision measurements of the pressure-volume relationship by Batlogg *et al.*³ determined the transition pressure P_c to be 5.0 kbar at room temperature. These measurements also showed that the high-pressure phase exhibits a large volume strain proportional to $(P - P_c)^{2/3}$. The volume strain was found to be anomalously large by comparison with other materials undergoing similar transformations.⁴ A consistent explanation for this observation is that the large volume strain results from buckling of the Re—O—Re bonds with the ReO_6 octahedra remaining rigid. Such rotations can be achieved by condensation of M_3 phonons because the atomic displacements for these phonons consist principally of coordinated rotations of the octahedra around $[100]$ axes. Assuming that the octahedra rotate as rigid units, the volume strain for small rotations should be proportional to ϕ^2 where ϕ is the rotation angle. One purpose of the present neutron diffraction measurements is to more explicitly establish that the angle of rotation of the ReO_6 octahedra is a valid order parameter for the transition.

The M_3 phonons are triply degenerate and the cubic

$Pm3m$ structure could therefore transform into $P4/mbm$, $I4/mmm$, or $Im3$ structures by condensation of one, two, or three M_3 phonons. $Im3$ was first suggested as the space group of the high-pressure phase of ReO_3 by Schirber and Mattheiss⁵ on the basis of several nonstructural investigations. A second purpose of the present measurements is to determine the structure(s) of the high-pressure phase(s) in ReO_3 and to determine whether more than one high-pressure phase exists.

Elastic neutron scattering measurements⁶ revealed superlattice reflections above P_c consistent with condensation of M_3 phonons. In addition, inelastic neutron scattering⁶ confirmed the existence of such a phonon mode whose frequency decreases dramatically as pressure approaches P_c from below. Both of these observations support the soft-mode mechanism for the transition as previously discussed. Additionally, both the P - V measurements³ and the elastic neutron scattering measurements⁶ indicated the possible existence of an intermediate phase between 5 and 5.3 kbar. Thus, the possible existence of more than one high-pressure structure, depending on the number of M_3 phonons that condense, was suggested.

The structure of the high-pressure phase at 15 kbar was recently established to be cubic $Im3$ by single-crystal neutron diffraction measurements performed by the time-of-flight Laue method.⁷ Unfortunately, data were collected at only one pressure. Thus, the pressure dependence of the structural distortion could not be established.

The powder neutron diffraction results reported in this paper establish the structural details of the phase transitions as a function of pressure and confirm the existence of at least two high-pressure phases. The M -point rotations are shown to be the only distortion associated with the transitions, with the rotation angle ϕ varying continuously through both phases even though the axis of rotation changes (discontinuously) from $[100]$ to $[111]$. For

the study of these transitions, neutron diffraction is particularly useful because of the relatively large cross section of oxygen. Thus, the rotations of the ReO_6 octahedra are much more easily seen with neutrons than with x rays. The use of the Rietveld method of structural refinement with high-resolution powder data offers a precision for atom positions comparable to that of the previously reported single-crystal neutron diffraction study and allows the pressure dependence of the distortion to be measured with sufficient accuracy to establish the order parameter exponent β where $\phi \propto (P - P_c)^\beta$ expresses the pressure dependence of the rotation angle.

EXPERIMENTAL PROCEDURE

Data were collected on the special environment powder diffractometer (SEPD) at the Intense Pulsed Neutron Source (IPNS) at Argonne National Laboratory.^{8,9} The sample was contained in a piston-in-cylinder pressure cell which has been described previously.^{10,11} The cell consists of an aluminum oxide cylinder supported by concentric steel binding rings. The sample is contained in a sealed Teflon tube with a hydrostatic liquid; Fluorinert FC-75 was used for this experiment. Previous work^{12,13} has shown that Fluorinert FC-75 remains hydrostatic to about 20 kbar and is reasonably soft and noncrystalline to higher pressures. The force is applied to the ends of the teflon tube through tungsten carbide pistons. Incident and scattered neutrons pass through windows in the steel. The SEPD allows data to be collected by the time-of-flight method at any fixed scattering angle from 12° to 157° . For this experiment, data were collected at 90° with right- and left-hand detector groups each covering solid angles of 0.022 sr. At the 90° scattering angle, the windows in the pressure cell provide sufficient collimation to prevent any cell Bragg scattering from appearing in the data. Since the windows are approximately 2.5 mm wide by 28.6 mm high, the effective sample volume is about 180 mm^3 . Data were collected for 30–40 h at each pressure. The ReO_3 sample was prepared by an iodine chemical transport reaction and was ground in a mortar and pestle under dry nitrogen before loading into the pressure cell.

The time-of-flight powder diffraction data were analyzed by the Rietveld method¹⁴ modified for time of flight.^{15,16} The pressures were determined by comparing the volumes deduced from the measured lattice spacings with those of the P - V measurements.³

Data collected at $P = 1$ bar and room temperature were refined in the $Pm3m$ space group. Both Re and O are in special positions ($1a$ and $3d$, respectively). From the point-group symmetries of these positions, Re has an isotropic temperature factor while O is anisotropic with two components, $\langle U_{\parallel}^2 \rangle$ and $\langle U_{\perp}^2 \rangle$, which represent vibrations parallel and perpendicular to the Re—O bond. The results of the refinement are in Table I. The refinement shows that the oxygen atoms have highly anisotropic thermal vibrations in a direction which is consistent with the soft M_3 phonon mode. The existence of a highly anisotropic anion Debye Waller factor is a common feature of perovskite-type structures, however, and is not neces-

TABLE I. Structural parameters for ReO_3 at atmospheric pressure in the cubic $Pm3m$ space group. Re is in special position $1a$ (0,0,0) and O is in special position $3d$ ($\frac{1}{2}$,0,0). Numbers in parentheses are standard deviations of the last significant digit.

$a = 3.7504(1) \text{ \AA}$
$\langle U^2 \rangle(\text{Re}) = 0.0023(4) \text{ \AA}^2$
$\langle U_{\parallel}^2 \rangle(\text{O}) = 0.0042(8) \text{ \AA}^2$
$\langle U_{\perp}^2 \rangle(\text{O}) = 0.019(5) \text{ \AA}^2$
$R_{\text{wp}} = 4.60\%$
$R_{\text{exp}} = 2.67\%$

sarily associated with a soft mode. The measured temperature factors are in good agreement with those obtained by single-crystal x-ray diffraction.¹⁷

The distorted perovskite structures can be derived from the $Pm3m$ structure by tilting the octahedra around the cubic axes. Glazer has compiled 23 different possible tilt arrangements.¹⁸ Any possible high-pressure phase could be described in terms of such tilt arrangements. From the initial refinements, it was evident that the relevant space groups for the high-pressure phases of ReO_3 are $P4/mbm$ and $Im3$, which are both consistent with M_3 phonon condensation. Data measured at $P \geq 7.3$ kbar could only be refined in the $Im3$ space group. Re and O are placed in the $8c$ and $24g$ special positions in the $Im3$ space group. Therefore, formally, Re has two and O has four thermal parameters. R -value ratio tests showed that the inclusion of these extra parameters could not be justified. Thus, the thermal ellipsoids were approximated by using the same anisotropic terms as for the $Pm3m$ phase. The refined atom positions were not significantly altered by this simplification. The results of the refinements in the $Im3$ structure are in Table II. It is significant to note that the anisotropy of the oxygen thermal ellipsoid is markedly reduced in the $Im3$ phase in comparison to that observed in the $Pm3m$ phase at ambient pressure. Figure 1 shows the $Im3$ unit cell, and Fig. 2 shows the measured and calculated powder profiles at $P = 17.25$.

The data at $P = 5.20$ kbar were refined in both the $P4/mbm$ and $Im3$ space groups; the results of the two refinements are in Table III. The $P4/mbm$ space group is tetragonal; the conventional setting with Re in the $2b$ positions and O in the $4h$ and $2a$ positions was used in the refinement. The unit cell in this setting has lattice constants $a' \simeq \sqrt{2}a$ and $c' \simeq a$, where a is the lattice constant for the $Pm3m$ unit cell.

A quantitative estimate of the statistical significance of refinements for different structural models can be made using R -value ratio tests such as those described by Hamilton.¹⁹ The weighted profile R values R_{wp} are correctly defined for use with standard R -value ratio tables²⁰ where the number of "free variables" (observations minus refinable parameters) is 865. (The small difference in the number of data for the $P4/mbm$ and $Im3$ models in Table III is caused by roundoff errors in defining the cutoffs at the edges of the peaks and is of no consequence.)

The refinements in the two space groups were done on the same experimental points to make a direct comparison

TABLE II. Structural parameters for ReO_3 versus pressure in the cubic $Im\bar{3}$ space group. Re is in special position $8c$ ($\frac{1}{4}, \frac{1}{4}, \frac{1}{4}$) and O is in special position $24g$ (0,y,z). Temperature factors are in units of \AA^2 .

P (kbar)	7.30	12.85	17.25	22.70	27.40
a (\AA)	7.4640(2)	7.4236(2)	7.3969(2)	7.3677(2)	7.3426(3)
$\langle U^2 \rangle (\text{Re})$	0.0022(5)	0.0018(5)	0.0015(5)	0.0012(6)	0.0016(6)
$y(\text{O})$	0.232(1)	0.225(1)	0.2197(8)	0.2158(9)	0.2104(9)
$z(\text{O})$	0.265(2)	0.273(1)	0.2763(9)	0.280(1)	0.281(1)
$\langle U_{\parallel}^2 \rangle (\text{O})$	0.006(1)	0.006(1)	0.005(1)	0.001(1)	0.0005(14)
$\langle U_{\perp}^2 \rangle (\text{O})$	0.0094(9)	0.007(1)	0.0077(9)	0.008(1)	0.009(1)
R_{wp} (%)	5.86	6.18	5.52	6.64	6.90
R_{exp} (%)	3.26	3.26	3.07	3.61	3.44

of weighted R values, R_{wp} , possible. This was done by excluding regions of data corresponding to some reflections from the $Im\bar{3}$ structure. Nine parameters were refined in both models. The ratio of R_{wp} for the two models is sufficient to favor the $P4/m\bar{3}m$ model at a 99.5% confidence level, even if over 20 additional variables were included in the model.²⁰ Thus, the $P4/m\bar{3}m$ structure is strongly favored by significance tests.

The $P4/m\bar{3}m$ refinement also yields a nonzero tetragonal strain. With the above-described setting of the unit cell, the tetragonal strain can be expressed as $\epsilon = \sqrt{2} - a/c$. The refinements showed minima with both positive and negative values of ϵ . The $P4/m\bar{3}m$ refinement described in Table III yields $\epsilon = -0.0015(2)$ and $R_{\text{wp}} = 5.196\%$, while the positive-strain refinement yields $\epsilon = 0.0012(3)$ and $R_{\text{wp}} = 5.213\%$. Thus, the negative strain is significantly favored. The presence of a negative strain implies a small but real distortion of the ReO_6 octahedra.

Distortion of the ReO_6 octahedron is allowed in both the $P4/m\bar{3}m$ and $Im\bar{3}$ structures. In $P4/m\bar{3}m$, two symmetry inequivalent Re—O bond lengths are allowed, while only one Re—O bond length exists in the $Im\bar{3}$ structure. In both structures, two inequivalent O—O distances (which are the edges of the ReO_6 octahedron) are present and provide a measure of the irregularity of the ReO_6 octahed-

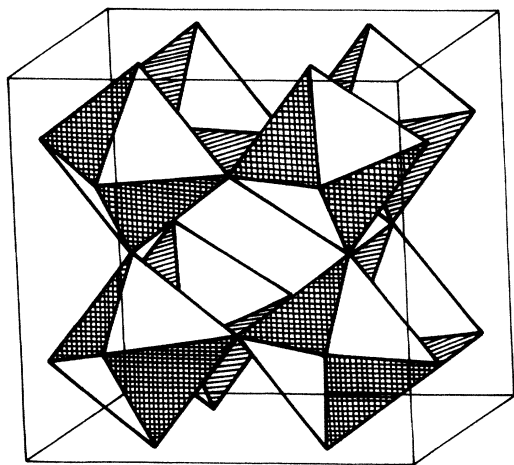


FIG. 1. $Im\bar{3}$ unit cell for ReO_3 . The ReO_6 octahedra are rotated around the $[111]$ direction which corresponds to a condensation of all three M_3 phonons.

ron. These Re—O and O—O distances versus pressure are given in Table IV. A plot of the O—O distances versus pressure in Fig. 3 shows that the distortion of the octahedron is small (within the uncertainties of the bond lengths) at all pressures. The difference between the two O—O distances at the highest pressure, 27.40 kbar, may be

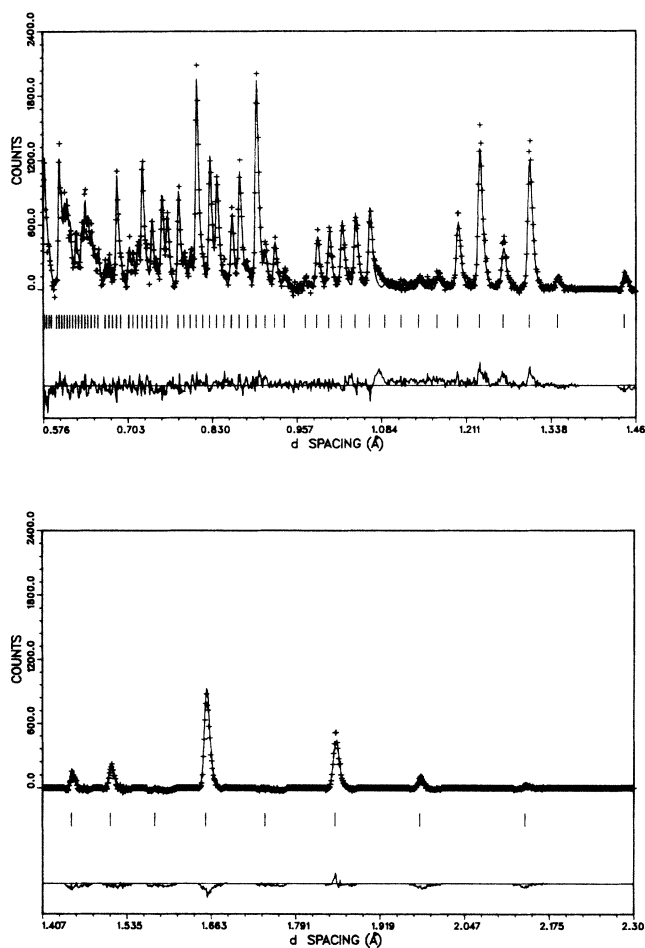


FIG. 2. Raw powder diffraction data (+) and calculated profile (solid line) for ReO_3 at 17.25 kbar. Tick marks below the profile indicate the positions of allowed reflections included in the calculation. A difference curve (observed minus calculated) appears at the bottom. Background has been subtracted before plotting.

TABLE III. Structural parameters for ReO_3 at 5.20 kbar in the tetragonal $P4/mbm$ and cubic $Im3$ space groups for refinements of identical data regions. The $P4/mbm$ space group yields a significantly lower R value. Temperature factors are in units of Å^2 .

Space group	$P4/mbm$	$Im3$
a (Å)	5.2968(5)	7.4882(2)
c (Å)	3.7415(6)	
$\langle U^2 \rangle(\text{Re})$	0.0027(4)	0.0019(4)
$x(\text{O})$	0.2368(8)	
$y(\text{O})$		0.241(3)
$z(\text{O})$		0.256(3)
$\langle U^2 \rangle(\text{O})$	0.0090(5)	0.0086(5)
R_{wp} (%)	5.196	5.322
R_{exp} (%)	2.945	2.940
No. of data	874	871
No. of parameters	9	9

an artifact of small systematic errors in the refinement resulting from nonhydrostatic conditions above 20 kbar and thus should not be considered a significant departure from the behavior observed at lower pressures.

A simple, physical explanation for the negative strain in the tetragonal phase can be given. When the ReO_6 octahedra rotate around the $[001]$ axis to form the $P4/mbm$ tetragonal phase, the Re—O bonds perpendicular to the rotation axis [$\text{Re—O}(1)$ in Table IV] relax to their ambient pressure lengths while the Re—O bonds parallel to the axis remain compressed and, in fact, are slightly shorter than the Re—O bonds which exist in the cubic phase at a pressure just below the transition at 5.0 kbar (approximately 1.872 Å). Thus, the negative strain results from the tendency for the bond lengths to assume their ambient-pressure values along those directions in which compression can be achieved by rotation of the octahedra. This hypothesis is further supported by the fact that the Re—O bond length in the cubic $Im3$ phase at 7.30 kbar is (within the errors bars) equal to that at ambient pressure and the bond compression is minimal (0.002 ± 1 Å) even at 27.40 kbar.

The $P4/mbm$ refinement of Table III was done with only one isotropic temperature factor for the two oxygen atoms in the $4h$ and $2a$ positions. A refinement with independent temperature factors for the two oxygen atoms yielded $\langle U_{2a}^2 \rangle = 0.007(5) \text{ Å}^2$ and $\langle U_{4h}^2 \rangle = 0.010(2) \text{ Å}^2$. This gives additional evidence that the refinement is comfortable with no static displacement of the $2a$ oxygen atoms, i.e., favors $P4/mbm$ over $Im3$. However, the ad-

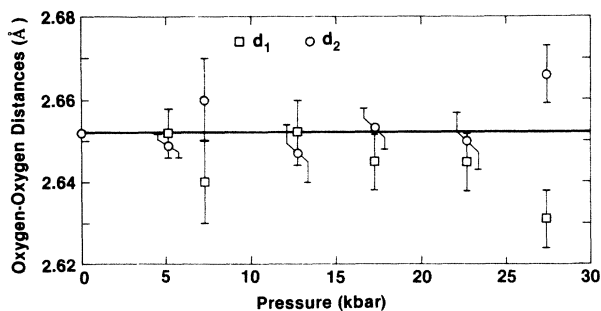


FIG. 3. Oxygen-oxygen distances in ReO_3 versus pressure. In the $P4/mbm$ and $Im3$ phases, there are two crystallographically inequivalent distances. The horizontal line is the O-O distance at ambient pressure.

dition of one more refinable parameter was not justified on the basis of R -value tests. Attempts to use $\langle U_{ij}^2 \rangle$'s with the actual site symmetry gave a lower R value, but large standard deviations on the $\langle U_{ij}^2 \rangle$'s. Moreover, no additional physical information was obtained with such a model. The rotation angle ϕ around the c axis was calculated to be $3.0(1)^\circ$ for the $P4/mbm$ data in Table III. ϕ correlates to a small extent with the thermal parameters and changes by about 0.5° when full $\langle U_{ij}^2 \rangle$'s are included in the model.

In addition to the Re—O and O—O distances, Table IV contains the rotation angle ϕ as a function of pressure. ϕ is calculated directly from the Re—O—Re bond angle in the $P4/mbm$ structure. For the $Im3$ structure, ϕ is calculated by projecting the oxygen atoms into a plane perpendicular to the $[111]$ axes. ϕ is therefore determined by the relation

$$\cos \phi = \frac{z + y}{2(z^2 + y^2 - zy)^{1/2}},$$

where y and z are the oxygen atom coordinates.

The rotation angle ϕ increases smoothly with increasing pressure above the transition and reaches a value of $14.0(3)^\circ$ at 27.40 kbar. Over this pressure range the changes in Re—O bond lengths and O—O distances across the edges of the ReO_6 octahedra are small (typically within the standard deviations). Thus, the structural distortion can be described to first order as a rigid rotation of the ReO_6 octahedra, i.e., the rotation angle ϕ is a suitable order parameter for the phase transitions.

The pressure dependence of the rotation angle is well described by a power law of the form $\phi \sim (P - P_c)^\beta$. ϕ versus pressure and the calculated curve based on this ex-

TABLE IV. Principal interatomic distances (Å) and angles (deg) in ReO_3 versus pressure. ϕ is the angle of rotation of the ReO_6 octahedra calculated as described in the text. Only the $P4/mbm$ structure at 5.20 kbar has two independent Re—O distances.

P (kbar)	0.001	5.20	7.30	12.85	17.25	22.70	27.40
$\text{Re—O}(1)$	1.875 20(5)	1.875(4)	1.874(1)	1.873(1)	1.8729(9)	1.872(1)	1.873(1)
$\text{Re—O}(2)$		1.8707(3)					
$\text{O—O}(1)$	2.651 93(7)	2.652(6)	2.64(1)	2.652(8)	2.645(7)	2.645(7)	2.631(7)
$\text{O—O}(2)$	2.651 93(7)	2.649(3)	2.66(1)	2.647(7)	2.653(6)	2.650(7)	2.666(7)
ϕ	0.0	3.0(1)	6.6(5)	9.5(3)	11.2(3)	12.6(3)	14.0(3)

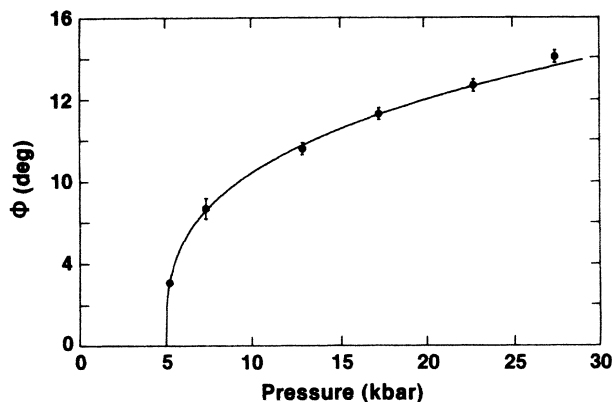


FIG. 4. Pressure dependence of the angle of rotation of the ReO_6 octahedra. The solid line shows the curve $\phi \propto (P - P_c)^\beta$ $\beta = 0.322(5)$.

pression are plotted in Fig. 4. The value of the exponent β was determined by linear regression from the slope of the $\ln \phi$ versus $\ln(P - P_c)$ curve, yielding a value of $\beta = 0.322(5)$. Within the uncertainties, ϕ appears to be a continuous function of pressure above 5 kbar, even though the direction of the rotation axis must change discontinuously from [100] to [111] at the transition from the $P4/mbm$ to the $Im3$ phase (5.3 kbar).

DISCUSSION

These results show that the phase transition in ReO_3 can be described by condensation of M -point phonons leading to rotation of the ReO_6 octahedra first around the [100] axis and, at higher pressures, around the [111] axis. The high-pressure phase is $Im3$ in agreement with recent single-crystal neutron diffraction results by Schirber *et al.*⁷

The existence of the tetragonal $P4/mbm$ phase in ReO_3 for a 300 bar wide region just above 5.0 kbar is now supported by the results of three independent experiments: the Rietveld refinement of powder data reported in this paper, single-crystal measurements of integrated intensities of the (200) and (310) Bragg peaks,⁶ and the precise dilatometric P - V measurements.³ The Rietveld refinements of the $P = 5.20$ -kbar data show that the $P4/mbm$ space group gives a statistically significant better refinement than the $Im3$ space group. In addition, a nonzero tetragonal strain is observed at 5.20 kbar. As an independent confirmation of the existence of the tetragonal phase at 5.20 kbar, the half widths of selected peaks were measured as a function of pressure. The tetragonal distortion would split or broaden: ($h00$) or ($h0l$) reflections while an (hhh) reflection would remain a singlet in the tetragonal phase. Measurements of the half widths of the (200) reflection at 0.001, 5.20, and 7.30 kbar showed that this reflection was broadened by 12% at 5.20 kbar. The (222) reflection showed no broadening at 5.20 kbar. Thus, the peak widths at 5.20 kbar give independent evidence that the phase at that pressure is tetragonal.

The single-crystal measurements⁶ showed an increase in the (200) intensity between 5 and 5.3 kbar, which was ex-

plained as a decrease in extinction originating from the tetragonal strain introduced by the transition into the $P4/mbm$ phase. The rocking curve of the (200) reflection was also consistently broader at pressures between 5.0 and 5.3 kbar than above 5.3 kbar. In addition, the intensity of the superlattice peak (310) showed a sharp and reproducible spike at $P \approx 5.3$ kbar. Batlogg *et al.*³ noted a small but distinct deviation from the otherwise highly accurate power-law behavior of the excess volume strain in the region from 5.0 to 5.3 kbar.

The oxygen-oxygen distances versus pressure plotted in Fig. 3 suggest that within the experimental uncertainty the ReO_6 octahedra rotate as rigid bodies. However, the sign of the tetragonal strain shows that this is not strictly true. Rigid-body rotations would give a positive strain in the $P4/mbm$ structure. The negative strain favored by the Rietveld refinement of the $P4/mbm$ structure indicates a slight distortion of the octahedra. The negative strain implies that the Re-O bonds perpendicular to the c axis are longer than the corresponding bond along the c axis. A possible explanation for this unexpected result is that the Re-O bond along the c axis remains in compression during the rotation of the ReO_6 octahedra, while the rotation relaxes the compression of the Re-O bond perpendicular to the c axis. Table IV shows that the $\text{Re-O}(1)$ bond lengths in the bent Re-O-Re bonds in both the $P4/mbm$ and $Im3$ structures are almost independent of pressure, while the $\text{Re-O}(2)$ bond, which is parallel to the rotation axis, is shortened in the $P4/mbm$ structure. All Re-O-Re bonds are bent in the $Im3$ structure. This means that in the $Im3$ phase, the anomalously large volume strain is achieved entirely through a bending of the Re-O-Re bonds with a minimal contribution from bond shortening.

The compression mechanism in ReO_3 is very similar to the one found in SiO_2 and other covalently bonded framework structures.²¹ SiO_2 consists of corner-linked tetrahedra. The predominant mechanism for the compression of SiO_2 is a cooperative rotation of the SiO_2 tetrahedra, while the Si-O bond length is unchanged.²¹ It should here be pointed out that ReO_3 is compressed via a shortening of the Re-O bond length below P_c . In the case of SiO_2 , the above-described compression mechanism works all the way down to ambient pressure.

As previously mentioned, the M_3 mode is triply degenerate and the pressure-induced phase transition can therefore be described by a three-component order parameter. Condensation of one, two, or three M_3 phonons can give rise to the sequence of phase transitions $Pm3m \rightarrow P4/mbm \rightarrow I4/mmm \rightarrow Im3$ which has been observed in Na_xWO_3 , a metallic perovskite compound which also shows M_3 phonon condensation upon cooling.^{4,22} The primary order parameter for the phase transition is a three-component order parameter which can be written as $\vec{\phi} = \phi \vec{e}$ where ϕ is the magnitude of the rotation angle and \vec{e} is a unit vector defining the direction of the rotation axis. $P4/mbm$, $I4/mmm$, and $Im3$ are all subgroups of $Pm3m$. A phase transition from $Pm3m$ to any of these space groups can therefore be of second order. From symmetry, however, transitions between $P4/mbm$, $I4/mmm$, and $Im3$ must be of first order. The first-

order nature results from the fact that once a rotation exists around a given axis, a transition to another rotation axis must involve discontinuous motion of the atoms. Discontinuities in the lattice constants during these transitions have been observed in Na_xWO_3 .^{4,22} In a similar manner, the nonzero tetragonal strain observed for ReO_3 at 5.20 kbar implies a discontinuity in the lattice parameter at 5.3 kbar where the $P4/mbm$ to $Im3$ transition occurs. The rotation angle in ReO_3 is surprisingly large, $14.0(3)^\circ$, at the highest measured pressure, 27.4 kbar. The corresponding angle in Na_xWO_3 is less than 6° . The empty A sites in ReO_3 apparently allow a less restricted rotation and are, in this way, responsible for the large compressibility of ReO_3 . In the case of Na_xWO_3 the order parameter was found to obey the power law $\phi \propto (T_c - T)^{1/2}$. The exponent of $\frac{1}{2}$ indicates that Na_xWO_3 obeys mean-field theory over the entire measured temperature range. Conversely, the measured value

for the exponent β which describes the pressure dependence of the order parameter in ReO_3 is 0.322(5) over the entire range of pressure. This could indicate an unusually large critical region extending to rotation angles of at least 14° or the proximity of a tricritical point. The observed value of β implies a novel restoring torque for the rotation which is almost perfectly quadratic, not linear, in ϕ . In both ReO_3 and Na_xWO_3 , ϕ is a continuous function of P (or T) despite the discontinuous changes in direction of the rotation axis associated with the first-order phase transitions. It is still an open question whether there is a narrow $I4/mmm$ intermediate phase in ReO_3 as in Na_xWO_3 .

ACKNOWLEDGMENTS

This work was supported by the U.S. Department of Energy, BES-Materials Sciences, under Contract No. W-31-109-ENG-38.

*Present address: The Studsvik Science Research Laboratory, S-611 82 Nyköping, Sweden.

¹F. S. Razavi, Z. Altounian, and W. R. Datars, *Solid State Commun.* **28**, 217 (1978).

²J. E. Schirber and B. Morosin, *Phys. Rev. Lett.* **42**, 1485 (1979).

³B. Batlogg, R. G. Maines, M. Greenblatt, and S. Di Gregorio, *Phys. Rev. B* **29**, 3762 (1984).

⁴R. Clark, *Phys. Rev. Lett.* **39**, 1550 (1977).

⁵J. E. Schirber and L. F. Mattheiss, *Phys. Rev. B* **24**, 692 (1981).

⁶J. D. Axe, Y. Fujii, B. Batlogg, M. Greenblatt, and S. Di Gregorio, *Phys. Rev. B* **31**, 663 (1985).

⁷J. E. Schirber, B. Morosin, R. W. Alkire, A. C. Larson, and P. J. Vergamini, *Phys. Rev. B* **29**, 4150 (1984).

⁸J. D. Jorgensen and J. Faber, Jr., in Argonne National Laboratory Report No. ANL-82-10, 1983, p. 105 (unpublished).

⁹J. M. Carpenter, G. H. Lander, and C. G. Windsor, *Rev. Sci. Instrum.* **55**, 1019 (1984).

¹⁰R. M. Brugger, R. B. Bennion, T. G. Worlton, and W. R. Meyers, *Trans. Am. Crystallogr. Assoc.* **5**, 141 (1969).

¹¹J. D. Jorgensen and T. G. Worlton, *J. Chem. Phys.* **83**, 329

(1985).

¹²D. L. Decker, S. Petersen, D. Debray, and M. Lambert, *Phys. Rev. B* **19**, 3552 (1979).

¹³J. D. Jorgensen and J. B. Clark, *Phys. Rev. B* **22**, 6149 (1980).

¹⁴H. M. Rietveld, *J. Appl. Crystallogr.* **2**, 65 (1969).

¹⁵R. B. von Dreele, J. D. Jorgensen, and C. G. Windsor, *J. Appl. Crystallogr.* **15**, 581 (1982).

¹⁶J. D. Jorgensen and F. J. Rotella, *J. Appl. Crystallogr.* **15**, 27 (1982).

¹⁷M. Morigana, K. Sato, J. Harada, H. Adachi, S. Ohba, and Y. Saito, *J. Phys. C* **16**, L177 (1983).

¹⁸A. M. Glazer, *Acta Crystallogr. Sect. A* **31**, 756 (1975).

¹⁹W. C. Hamilton, *Acta Crystallogr.* **18**, 502 (1965).

²⁰*International Tables for X-Ray Crystallography* (Kynoch, Birmingham, England, 1974), Vol. IV, see Table 4.2, pp. 288–292.

²¹L. Cartz and J. D. Jorgensen, *J. Appl. Phys.* **52**, 236 (1981); and J. D. Jorgensen, *ibid.* **49**, 5473 (1978).

²²M. Sato, B. H. Grier, G. Shirane, and T. Akahane, *Phys. Rev. B* **25**, 6876 (1982).